

Estimation of Sentiment Effects in Financial Markets: A Simulated Method of Moments Approach

Zhenxi Chen¹ · Thomas Lux^{2,3}

Accepted: 16 November 2016 / Published online: 28 November 2016
© Springer Science+Business Media New York 2016

Abstract We take the model of Alfarano et al. (J Econ Dyn Control 32:101–136, 2008) as a prototype agent-based model that allows reproducing the main stylized facts of financial returns. The model does so by combining fundamental news driven by Brownian motion with a minimalistic mechanism for generating boundedly rational sentiment dynamics. Since we can approximate the herding component among an ensemble of agents in the aggregate by a Langevin equation, we can either simulate the model in full at the micro level, or via an approximate aggregate law of motion. In the simplest version of our model, only three parameters need to be estimated. We explore the performance of a simulated method of moments (SMM) approach for the estimation of this model. As it turns out, sensible parameter estimates can only be obtained if one first provides a rough “mapping” of the objective function via an extensive grid search. Due to the high correlations of the estimated parameters, uninformed choices will often lead to a convergence to any one of a large number of local minima. We also find that the efficiency of SMM is relatively insensitive to the size of the simulated sample over a relatively large range of sample sizes and the SMM estimates converge to their GMM counterparts only for large sample sizes. We believe that this feature is due to the limited range of moments available in univariate asset pricing models, and that the sensitivity of the present model to the specification of

Electronic supplementary material The online version of this article (doi:[10.1007/s10614-016-9638-4](https://doi.org/10.1007/s10614-016-9638-4)) contains supplementary material, which is available to authorized users.

✉ Thomas Lux
lux@economics.uni-kiel.de

¹ School of Economics and Commerce, South China University of Technology, Guangzhou, China

² Department of Economics, University of Kiel, Kiel, Germany

³ Bank of Spain Professor in Computational Economics, Department of Economics, University Jaume I, Castellon, Spain

the SMM estimator could carry over to many related agent-based models of financial markets as well as to similar diffusion processes in mathematical finance.

Keywords Simulation-based estimation · Herding · Agent-based model · Model validation

JEL Classification C14 · C15 · F31

1 Introduction

By taking into account features such as the existence of heterogeneous agents with different trading strategies, bounded rationality or interactions among agents, behaviorally motivated models of financial markets have undergone a burgeoning development over the past two decades. Quite a number of these models are able to replicate and, therefore, explain the documented stylized facts of financial markets, including fat tails and temporal dependence of volatility. Recent surveys of this literature can be found in [Hommes \(2006\)](#), [LeBaron \(2006\)](#) and [Lux \(2009b\)](#) among others.

This literature got started by [Day and Huang \(1990\)](#) who model a market populated by fundamentalists and chartists to study randomly alternating bullish and bearish market episodes. [Kirman \(1993\)](#), [De Grauwe et al. \(1995\)](#) and [Lux \(1995\)](#) add further aspects of traders' interactions such as herd behavior and switching of strategies and already make first attempts to explain selected stylized facts. [Brock and Hommes \(1998\)](#) initiated a related strand of literature based upon a discrete choice framework for agents' choice of strategies. [Chiarella and He \(2002\)](#) additionally allow agents to have different risk attitudes within such a setting.

Most of this literature uses simulations to explain some of the stylized facts based on complex nonlinear models. [Alfarano and Lux \(2007\)](#) and [Alfarano et al. \(2008\)](#) are among the few exceptions. They derive analytical solutions for the time-variation of higher moments and related measures of the stylized facts, enabling them to determine the conditions under which these particular features arise. [Alfarano and Lux \(2007\)](#) derive closed form solutions of variance and kurtosis of the return distribution of their model based upon the unconditional distribution of an index of the average expectations of their boundedly rational agents. In their setting, expectation formation is formalized via Kirman's (1993) seminal "ant" model for the herding interactions among agents. [Alfarano et al. \(2008\)](#) further incorporate autonomous changes of sentiment into the dynamics of agents' interactions, in addition to the herding mechanism. They also derive approximate closed form solutions of autocorrelation functions. In a companion paper to ours, [Ghoshghadze and Lux \(2016\)](#) derive higher-order approximations for the same moments and explore their applicability in a generalized method of moments (GMM) setting. This paper uses the model of [Alfarano et al. \(2008\)](#) to explore the issue of efficiency of estimation of such a model via the simulated method of moments (SMM) approach.

The robustness of the theoretical models in generating empirical "stylized facts" inspires the empirical application and validation of agent based models. Since much of this literature is based on simulation, the use of simulated moments seems tailor-made

for bringing these models to the data. Simulated method of moments has been proposed initially by [McFadden \(1989\)](#), [Pakes and Pollard \(1989\)](#), [Lee and Ingram \(1991\)](#) and [Duffie and Singleton \(1993\)](#). SMM or closely related approaches have been applied in a variety of settings. [Molina et al. \(2005\)](#) use SMM to estimate behavioral parameters in a model of a transportation network. [Rahmandad and Sabounchi \(2012\)](#) apply SMM to investigate population obesity dynamics. [Ruge-Murcia \(2007\)](#) estimates a dynamic stochastic general equilibrium model (DSGE) using SMM. [Grammig and Schaub \(2014\)](#) combine GMM and SMM in estimating an asset pricing model, combined with a DSGE model of the underlying fundamental dynamics.

In a context closely related to ours, [Gilli and Winker \(2003\)](#) already developed a non-linear optimization technique combining the Nelder–Mead and a threshold acceptance algorithm to estimate Kirman’s “ant” model. [Winker et al. \(2007\)](#) propose a criterion function based on moments related to the stylized facts to assess the empirical application of agent based models. [Franke \(2009\)](#) applies such an objective function within an SMM framework to estimate the model of [Manzan and Westerhoff \(2005\)](#). [Franke and Westerhoff \(2011\)](#) also adopt SMM to estimate a structural stochastic volatility model, but instead of the standard SMM setting of [Duffie and Singleton \(1993\)](#) use a bootstrap method for generating the weighting matrix of their moments. [Franke and Westerhoff \(2012, 2016\)](#) continue this line of research by estimating different “reduced” types of simple agent-based models and comparing their capability to explain the stylized facts. [Grazzini and Richiardi \(2015\)](#) illustrate the application of SMM to an agent-based framework via Monte Carlo simulations for a simple model of price formation in a double auction. [Jang \(2015\)](#) uses SMM to estimate the parameters of the model of [Alfarano and Lux \(2007\)](#). He reports a variety of hurdles in the SMM approach such as a rugged and possibly very flat surface of the objective function and difficulty to obtain unique parameter estimates from different initial conditions. Similar problems are also highlighted in a different context by [Grammig and Schaub \(2014\)](#) who point to principal limitations of an SMM approach in the presence of small datasets used to estimate complex theoretical models.

Alternative minimum distance estimation different from GMM/SMM have been proposed by [Lamperti \(2015\)](#) and [Barde \(2016\)](#). Both approaches are based on information-theoretic measures. [Barde \(2016\)](#) is particularly close to the present context in that he compares three agent-based models of herding in financial markets that are close in spirit to our prototype model. While he does not estimate the parameters of these models directly, he compares the performance of a large set of parametric specifications of these models and determines the model confidence set (models that cannot be significantly outperformed by others) among the agent-based and a variety of GARCH time series models. As it turns out, among the three agent-based models, the one by [Franke and Westerhoff \(2016\)](#) most often appears in model confidence sets for different data while the competitor proposed by [Alfarano et al. \(2005\)](#)—a close cousin of the model used here—is a close second.

Most of the other applications, however, confine themselves to estimate the parameters of agent based models, without systematic exploration of the performance of their estimation algorithms. While one finds a variety of simulation studies on all types of models and estimation methods in the econometrics literature, not too much evidence on the performance of SMM estimation is available. One obvious reason is

certainly the computational effort involved in executing such a study that amounts to assessing the performance of simulated moments via simulations. We here attempt to close this particular gap in the literature by more systematically exploring the performance of SMM estimation via Monte Carlo simulations using the prototype simple agent-based model of [Alfarano et al. \(2008\)](#) for an exemplary case study. The model allows for two different scenarios: a bimodal and unimodal distribution of the sentiment index. It is shown that strong interpersonal communication corresponding to the bimodal distribution typically matches best the empirical data. As this model matches the most prevalent stylized facts, it should be observationally equivalent to a number of alternative specifications. As an added advantage and in contrast to many related models, analytical moment conditions (at least approximate ones) exist for this model so that we can compare the performance of SMM to a generalized method of moment (GMM) estimator developed in a companion paper ([Ghoshadze and Lux 2016](#)). The availability of GMM results provides the opportunity to compare the performance of SMM and GMM for the very same setting, and, therefore, allows an assessment of the relevance of the additional noise induced by simulations. As we will see, this comparison turns indeed out to reveal a relatively slow convergence of the SMM estimates to their GMM counterparts even for relatively sizable simulated samples. Another contribution of this paper is the development of a systematic approach to handle estimation problems with multiple minima and discontinuous gradients of the objective function. It is found that performing a systematic “mapping” of the objective function via an extensive grid search is a very useful first step for determination of sensible initial conditions to start an optimization algorithm for local fine-tuning of parameter estimates. As concerns the details of the SMM estimator, we find that many other variations of our setting (using different moments, adopting different weighting matrices) have very little influence on the quality of our estimates. We also find that the variability of our estimates decreases more slowly with empirical sample size than expected, and that the estimation errors are not very sensitive to the simulated sample size over a broad range of feasible choices.

The rest of the paper is organized as follows. Section 2 introduces the theoretical model that basically boils down to a diffusion process of an asset price that combines fundamental factors and sentiment dynamics. Section 3 develops the methodology. After illustrating the surface properties of the objective function, we conduct Monte Carlo simulations to compare the performance of different sets of moments and other variations of the SMM designs. Section 4 applies the developed methodology to estimate the parameters of this behavioral model using a broad selection of empirical high-frequency data. Lastly, Sect. 5 concludes the paper.

2 Theoretical Model

In our financial market model, the log price and log fundamental value at time t are denoted by p_t and F_t . There are two groups of investors: fundamentalists and noise traders. The fundamentalist group has N_f members with average trading volume V_f . Fundamentalists invest based on the price deviation from the fundamental value. They purchase under-valued assets and sell over-valued ones. Their excess demand, then, amounts to

$$D^f = N_f V_f (F_t - p_t). \quad (1)$$

The log fundamental value, F_t is assumed to follow Brownian motion without a drift, so that over finite time intervals, the fundamental value at time $t + \Delta t$ follows a Normal distribution $(F_{t-1}, \sigma_f \Delta t)$. For a unit time change (i.e., daily data), $\Delta t = 1$, this setting is equivalent to a random walk process characterizing the fundamentals:

$$F_{t+1} = F_t + \sigma_f \cdot e_t, \quad (2)$$

where σ_f is the standard deviation of the innovations of the fundamental value and $e_t \sim iidN(0, 1)$.

The group of noise traders consists of a finite number of agents N_c , each of them being in either state 1 or 2, the optimistic or pessimistic state. Agents will buy or sell V_c units of the asset if they are in state 1 or 2, respectively. The number of agents in the optimistic state is denoted by n_t . Define the population configuration: $x_t = 2n_t/N_c - 1$, which signals a balanced disposition if equal to zero and amounts to optimistic or pessimistic majorities if positive or negative. The process of agents' change of opinion is, in general, also formulated in continuous time. A noise trader can switch between the optimistic and pessimistic states. The herding dynamics is characterized by time-varying transition rates for a pessimistic trader to become an optimistic one ($\pi_{x,t}^+$) and vice versa ($\pi_{x,t}^-$). The transition rates are given by combinations of autonomous switches of opinion (happening with a Poisson intensity a) and switches brought about by pair-wise communication (happening with a rate b that has to be multiplied with the probability of being paired with an agent of the opposite opinion). Formally, this amounts to:

$$\begin{aligned} \pi_{x,t}^+ &= (N_c - n_t) (a + bn_t) = (1 - x_t) [2a/N_c + b(1 + x_t)] N_c^2, \\ \pi_{x,t}^- &= n_t (a + b(N_c - n_t)) = (1 + x_t) [2a/N_c + b(1 - x_t)] N_c^2. \end{aligned} \quad (3)$$

As shown by [Alfarano et al. \(2008\)](#), the temporal development of the probability density of x_t , $\omega(x)$, is characterized by the Fokker–Planck or forward Kolmogorov equation:

$$\frac{\partial \omega(x, t)}{\partial t} = \frac{\partial}{\partial x} (A(x) \omega(x, t)) + \frac{1}{2} \frac{\partial^2}{\partial x^2} (D(x) \omega(x, t)) \quad (4)$$

with drift and diffusion terms: $A(x) = -2ax$, $D(x) = 2b(1 - x^2) + 4a/N_c$. As a consequence, the macroscopic dynamics of the agent-based model can be approximated by a continuous-time diffusion process \tilde{x}_t :

$$d\tilde{x}_t = A(\tilde{x}_t) dt + \sqrt{D(\tilde{x}_t)} dB_t \quad (5)$$

with B_t standard Brownian motion, and $A(\cdot)$ and $D(\cdot)$ the drift and diffusion defined above. [Ethier and Kurtz \(1986\)](#) show that this approximation obeys:

$$\sup_{t \leq T} |x_t - \tilde{x}_t| \leq \Gamma_{N_c}^T \frac{\log N_c}{N_c}$$

with $\Gamma_{N_c}^T$ a random variable which decays asymptotically as N_c^{-2} . Note that the quality of the approximation as derived by the above formula indicates that with the high number of agents we typically see interacting in financial markets, the discrepancy between x_t and \tilde{x}_t should be negligible. When using Eq. (5) for simulation, the diffusion approximation needs to be discretized with a sufficiently small increment Δt_0 to not jeopardise its proximity to the true agent based model (ABM). In this paper we will, however, perform Monte Carlo exercises and empirical applications using an exact discrete-event simulation for our agent-based model. In a working paper version we have used the diffusion approximation but curiously enough the approximation is more time consuming than the exact simulation. As a consequence, the limited amount of Monte Carlo runs provided less sharp conclusions than in the present version.

The discrete-event simulation of the asynchronous continuous-time framework of agents' change of opinion works as follows: the Poisson transition rates defined in Eq. (3) imply that the waiting times of individual agents follow exponential distributions with parameters $1/\pi_{x,t}^+$ or $1/\pi_{x,t}^-$, depending on their current state. Since the minimum of independently exponentially distributed variables also follows an exponential distribution with its parameter equal to the sum of the individual parameters, the minimum waiting time is exponentially distributed with parameter $\lambda = n_t \pi_t^- + (N_c - n_t) \pi_t^+$. Hence, the time of the next change of any agent can be determined by a random draw from such an exponential distribution. In a second step, a uniform random draw determines whether the change has been of an optimistic agent switching to the pessimistic mode or vice versa which happens with probabilities $n_t \pi_t^- / \lambda$ and $(N_c - n_t) \pi_t^+ / \lambda$, respectively. We record the changes with their pertinent time stamps of this stochastic process until we have surpassed the scheduled time horizon T of a simulation (plus a transient to allow the system to converge to its ergodic distribution) and extract the trajectories $\{x_t\}_{t=1}^T$ as the realization of the configuration of agents' opinions at any integer time step. The discretized series is used to determine the usual price dynamics which is also extracted at discrete intervals.

The time varying x_t affects the excess demand of noise traders according to

$$D^c = N_c V_c x_t. \quad (6)$$

with V_c the constant trading volume of each noise trader. Under a standard Walrasian price adjustment mechanism, price changes depend on the overall excess demand:

$$\begin{aligned} \frac{dp}{dt} &= \beta (D^f + D^c) \\ &= \beta [N_f V_f (F_t - p_t) + N_c V_c x_t]. \end{aligned} \quad (7)$$

Assuming instantaneous market clearing with $\beta \rightarrow \infty$, we derive the equilibrium market price driven by the fundamental price and the population configuration of noise traders at time t ,

$$p_t = F_t + \frac{N_c V_c}{N_f V_f} x_t. \quad (8)$$

Over discrete time intervals, returns can be defined as log price changes. Assuming trading in continuous time, we should, in principle, have considered all the different

configurations of x_t that it had been passing through between any period in time t and $t + 1$. We neglect this complication in the following as it has no effect on the appearance of the discretely recorded time series, and let returns just be governed by the discrete change of x_t between integer time steps:

$$\begin{aligned} r_{t+1} &= p_{t+1} - p_t \\ &= F_{t+1} - F_t + \frac{N_c V_c}{N_f V_f} (x_{t+1} - x_t) \\ &= \sigma_f \cdot e_t + \frac{N_c V_c}{N_f V_f} (x_{t+1} - x_t). \end{aligned} \quad (9)$$

This means that returns are determined by the changes of the fundamental value and the change in noise traders' behavior. Note that this equation could also be seen as a generalization of previous time series models that have introduced sentiment as a linear risk factor in otherwise standard asset pricing models (e.g. [Brown and Cliff 2004](#)). Here, we estimate a model with a nonlinear sentiment component.

It is interesting to note that the herding process, Eq. (5) has a mean-reverting drift just because the opinion index is a bounded stochastic process so that any wave of optimistic or pessimistic sentiment will eventually find its end. The nonlinear diffusion shows that for b relatively high compared to a the random variation would slow down in the presence of a strong positive or negative majority, $x \rightarrow \pm 1$. This shows the persistence of majority opinions that is caused by interpersonal communication reinforcing an existing dominance of one opinion over the other. For $b > a$, the agent-based system and its diffusion approximation are characterized by a bimodal distribution of the opinion index x_t . For weaker interpersonal influence, $a > b$, the distribution is unimodal and centered at $x_t = 0$.

3 Simulated Method of Moments Estimation

For the quantitative analysis of a return time series r_t with length T , several elementary statistics or moments are typically used. These moment statistics include the second and fourth moment of returns ($E(r^2)$ and $E(r^4)$) as well as the autocovariance of both raw returns and certain higher powers, e.g., squared returns, at various lags. For univariate asset prices, these conditional and unconditional moments provide the range of inputs one could use in any estimation based on moment matching. At the same time, these moments are quantitative measurements of the well-known stylized facts of fat tails and volatility clustering so that they should be in the center of interest for any model that attempts to explain these salient features. In our estimation approach, we stack the moments of interest in a vector $m = (m_1, \dots, m_n)'$. For an L -sample of returns r_t , define the compact variable $z_t = (r_t, r_{t-1}, \dots, r_{t-L})$. Moments for (pseudo-)empirical data are computed as the time average

$$m^{emp} = (1/T_{emp}) \sum_{t=1}^{T_{emp}} m(z_t^{emp}). \quad (10)$$

Similarly, moments of the simulated data can be computed as

$$m^{sim} = (1/T_{sim}) \sum_{t=1}^{T_{sim}} m \left(z_t^{sim}(\theta, \varepsilon_t) \right). \quad (11)$$

with $\theta = (a, b, \sigma_f)$ the vector of parameters that we attempt to estimate, and ε_t the joint influence of the Wiener processes governing the fundamental factor and the stochastic elements of the agent-based process of sentiment formation. These processes do, in fact, not only enter via the time t realization, but also via the change of sentiment between time $t - 1$ and t in our discrete event simulation, but we summarize all stochastic factors that play a role between time $t - 1$ and time t by ε_t . The length of the simulated data T_{sim} can be arbitrarily long depending on the budget of computing time. Usually, it should in any case be longer than T_{emp} such that the ratio of the simulated length to the empirical one, $R = T_{sim}/T_{emp}$ with $R \geq 1$.

The simulated moments m^{sim} are a function of θ . Moment matching requires that $h_T = m^{emp} - m^{sim}$ should be minimized and as a result, parameter estimates $\hat{\theta}$ can be obtained as

$$\hat{\theta}_T = \arg \min_{\theta} \left(h_T(\theta)' W_T h_T(\theta) \right), \quad (12)$$

where W_T is a positive definite and possibly random weighting matrix which should reflect the different degrees of precision in the measurement of the different moments. Lee and Ingram (1991) and Duffie and Singleton (1993) show that under general regularity conditions, the SMM estimator for θ is asymptotically consistent.

The most efficient estimator is obtained with the choice of W_T as the inverse of an unbiased and efficient estimator of the variance–covariance matrix of the moment conditions $h_T(\theta)$. A standard estimator would, for instance, be the Newey–West estimator

$$\begin{aligned} \hat{\Omega} &= \Gamma_0 + \sum_{j=1}^p \left(1 - \frac{j}{p+1} \right) (\Gamma_j + \Gamma_j'), \\ \text{with } \Gamma_j &= \frac{1}{T} \sum_{t=j+1}^T h_{T,t}(\theta) h_{T,t-j}(\theta)', \\ h_{T,t}(\theta) &= m(z_t^{emp}) - \frac{1}{T_{sim}} \sum_{t=1}^{T_{sim}} m(z_t^{sim}(\theta, \varepsilon_t)). \end{aligned} \quad (13)$$

The weighting matrix W_T is obtained as the inverse of the Newey–West estimator

$$W_T = \left(\left(1 + \frac{1}{R} \right) \hat{\Omega} \right)^{-1}, \quad (14)$$

where the factor $\frac{1}{R}$ captures the additional variability for the simulation of moments compared to the use of analytical moments in a GMM estimation.

Franke and Westerhoff (2016) propose as an alternative that the weighting matrix W_T can be obtained through bootstrapping of the moments in the empirical data. Experimenting with this choice, we obtained results that were inferior to the standard choice of the inverse variance–covariance matrix. Since a bootstrapped weight matrix does not amount to efficient estimation of the covariance matrix of the moment estimates, care would also have to be taken with the asymptotic distribution of the resulting parameter estimates.

Note that our model should obey standard “regularity conditions” for GMM and SMM estimation. First, the agent-based process is Markovian, strictly stationary and ergodic. We can, in fact, derive its asymptotic distribution and at least compute approximations to various moments that can be used to also arrive at approximate moment conditions for the process governing returns. Note, however, that our process has a limiting case that would not obey standard regularity conditions. If we let $N_c \rightarrow \infty$, in the bimodal case, $b > a$, all probability mass would become concentrated at the boundaries of the support of x_t , i.e. -1 or $+1$, and hence, positive recurrence of the Markov chain would cease to prevail in this limit. This can also be seen in the diffusion approximation where the diffusion term would converge to $2b(1 - x_t^2) = 0$ at $x_t = \pm 1$ so that any trajectory would either get stuck at $x_t = -1$ or $x_t = 1$ as absorbing boundaries. It is actually known that the stochastic differential equation that represents the “reduced form” of our ABM in the limit of an infinite number of agents is non-ergodic for $b > a$ (Larsen and Sørensen 2007), but assuming any finite number of agents version of the model saves us from this inconvenient scenario. Of course, with a very large number of agents, we might get very close to the limiting case in the sense that the process might for very long time be trapped in the vicinity of one of its outer borders. We, therefore, choose a “moderate” number of agents, $N_c = 100$, in our further exploration.¹ Figure 1 shows that in this case, the agent-based process explores the whole support of x_t and switches repeatedly between optimistic and pessimistic majorities. The figure also illustrates that these switches are responsible for phases of high and persistent volatility, i.e., the emergence of the stylized facts. The lower panels of Fig. 1 show that highly positive (negative) values of sentiment come along with high (low) realizations of log market prices. This relationship is, however, far from linear since prices also react to fundamental news. The scatter plot of returns versus x_t indicates that the highest realizations of returns are observed when sentiment is not too extreme. The reason is that in such a situation, fluctuations are more pronounced as there is no dominating opinion among noise traders.

In the Appendix 2, we report tests for stationarity and ergodicity of our simulated returns series following the approach of Grazzini (2012). It turns out, that the test for ergodicity rejects its null hypothesis very rarely for all the moments used in the subsequent analysis, while rejection or not of stationarity depends on the sample size. In particular, all moments related to volatility (squared returns, fourth moment,

¹ Lux (2009a) estimates a related model directly for a sentiment index of the German economy, and finds that the behavior of the index can be well reproduced once one allows for an “effective” number of agents that is smaller than the notional one. He justifies this adjustment by agents being not as autonomous as the basic model assumes, but actually belonging to a limited number of groups with relatively uniform behavior and interaction in the sense of Eq. (3) occurring between these groups.

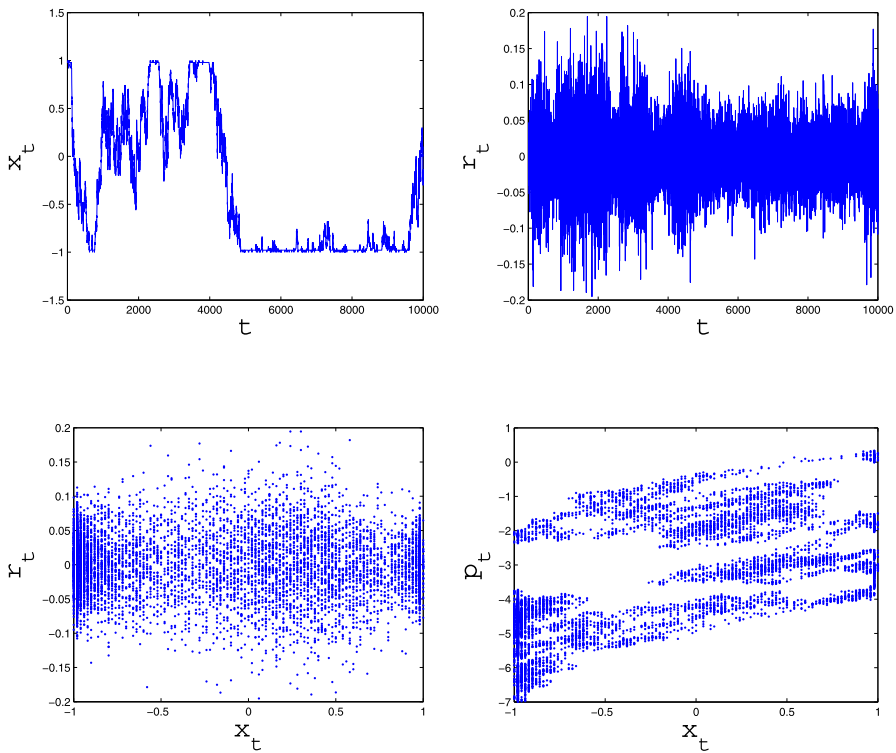


Fig. 1 Trajectories of the opinion index, x_t and returns, r_t as well as plots r_t versus x_t and p_t versus x_t . The underlying parameters of this simulation are $a = 0.0003$, $b = 0.0014$, $\sigma_f = 0.03$. This implies that the stationary distribution of the sentiment process would be bimodal

autocovariances of squared returns) are diagnosed to be stationary only for sufficiently long series. This finding is indicative of relatively long dependence in all measures of volatility—a feature that is also pervasive in empirical asset returns.

3.1 Smoothness of the Objective Function

Before we proceed to developing the estimation methodology, we first conduct a preliminary check of the sensitivity of the moments with respect to the model parameters and investigate the properties of the surface of the objective function. Based on [Alfarano et al. \(2008\)](#), $a > b$ implies the dominance of autonomous sentiment changes of noise traders over their herding tendency, leading to unimodality of the unconditional distribution of the index x with a peak at $x = 0$. On the other hand, $a < b$ leads to a bimodal distribution of x . We distinguish between these two settings in checking the smoothness of the objective function. In the following, we choose $(a, b) = (0.0003, 0.0014)$ and flipped values $(a', b') = (0.0014, 0.0003)$ to represent the bimodal and unimodal setting, respectively. Table 1 lists the default parameter setting for our pseudo-empirical model to generate price trajectories. The moment conditions adopted in our evaluations are: unconditional second and fourth moment,

Table 1 Parameters for price trajectories simulation

	N_c	T_{emp}	T_{sim}	$\frac{N_c V_c}{N_f V_f}$	σ_f	a	b
Bimodal	100	5000	20,000	1	0.03	0.0003	0.0014
Unimodal	100	5000	20,000	1	0.03	0.0014	0.0003

first-order autocovariance of raw returns, as well as autocovariances of squared and absolute returns at lags 1, 5, 10, 15, 20 and 25. Note that in this way we capture both excess kurtosis and dependency in higher moments, and a small (negative) autoregressive dependency of raw returns is also in harmony with most empirical findings for high frequency financial data. Also note that for all the trajectories of this paper, by default the first 5000 periods are discarded to remove the transient phase. The iteration length T_{emp} is the length of the pseudo-empirical time series that we generate in our Monte Carlo experiments. We generate the moments m^{emp} and the weighting matrix W based on the simulated price trajectories. We set $\theta = (a, b, \sigma_f)$ as parameters to be estimated. Suppressing the influence of the factor $\frac{N_c V_c}{N_f V_f}$ in Eq. (9) by setting it equal to unity is a consequence of our experience (detailed below) of the simple setting with three parameters only, $\theta = (a, b, \sigma_f)$. As it turns out, even in this case we do have to cope with the issue of weak identification due to high correlations of our parameters. Adding $\frac{N_c V_c}{N_f V_f}$ as a fourth parameter would deteriorate results by so much that the outcomes of our estimation would become almost useless. However, we can interpret $\frac{N_c V_c}{N_f V_f}$ as a scale factor that can be approximately factored out (in fact, due to obvious collinearity, we could at best estimate only the composite parameter $\frac{N_c V_c}{N_f V_f}$, but this composite parameter is not exactly collinear to any other parameter).

As a starting step to our subsequent exploration of parameter estimation, we investigate how sensitive the chosen moments are to variations of the model parameters. To assess the effect of changing parameters, we have conducted in each case 100 Monte Carlo runs with 20,000 observations (after discarding a transient of 5000 data points) with identical initial conditions, and report the effect of changes by 25% of each one of the parameters, respectively. The entries of the table are the relative changes of the pertinent moment under a change of 25% of the relevant parameter. We can see from Table 2 that all changes of parameters lead to changes of moments of various magnitudes. Hence, our moment conditions are sensitive with respect to the underlying parameters. Most of the moments are most sensitive to σ_f under both the bimodal and unimodal setting, and least so with respect to b and a under the bimodal and unimodal scenarios, respectively, which might indicate that we should expect different degrees of precision in their estimation. Indeed, a seems to exert very little effect on most moments in the unimodal regime, and we will find later that its estimation comes with a particularly high bias and variance in this case. Other critical points could be high simulation variance of the autocovariance of raw returns and the largely similar reaction of the autocovariance of squared return and the fourth moment to variations of the parameters. A relatively narrow range of variations is also found for the autocovariances of absolute returns and it remains to be seen whether the various

Table 2 Sensitivity (relative changes) of moments to parameter changes of 25% evaluated with 100 Monte Carlo runs

	Bimodal setting			Unimodal setting		
	a	b	σ_f	a	b	σ_f
$m_1 = E(r_t^2)$	0.08 (0.05)	0.03 (0.03)	0.29 (0.03)	0.02 (0.01)	0.08 (0.01)	0.34 (0.00)
$m_2 = E(r_t r_{t-1})$	-2.77 (17.52)	-0.31 (21.06)	-0.10 (8.53)	-0.65 (8.19)	0.41 (14.89)	0.07 (1.69)
$m_3 = E(r_t^2 r_{t-1}^2)$	0.15 (0.11)	0.16 (0.08)	0.51 (0.05)	0.04 (0.03)	0.18 (0.04)	0.79 (0.01)
$m_4 = E(r_t^4)$	0.14 (0.11)	0.16 (0.08)	0.50 (0.05)	0.03 (0.03)	0.18 (0.04)	0.77 (0.01)
$m_5 = E(r_t r_{t-1})$	0.08 (0.05)	0.03 (0.03)	0.30 (0.03)	0.02 (0.01)	0.08 (0.02)	0.35 (0.00)
$m_6 = E(r_t^2 r_{t-5}^2)$	0.15 (0.11)	0.16 (0.09)	0.51 (0.06)	0.03 (0.03)	0.17 (0.03)	0.79 (0.01)
$m_7 = E(r_t r_{t-5})$	0.08 (0.05)	0.03 (0.04)	0.30 (0.03)	0.02 (0.01)	0.08 (0.01)	0.35 (0.00)
$m_8 = E(r_t^2 r_{t-10}^2)$	0.15 (0.11)	0.15 (0.09)	0.52 (0.06)	0.04 (0.03)	0.17 (0.04)	0.79 (0.01)
$m_9 = E(r_t r_{t-10})$	0.08 (0.05)	0.03 (0.04)	0.30 (0.03)	0.02 (0.01)	0.08 (0.01)	0.35 (0.00)
$m_{10} = E(r_t^2 r_{t-15}^2)$	0.15 (0.11)	0.16 (0.09)	0.52 (0.06)	0.04 (0.03)	0.17 (0.04)	0.79 (0.01)
$m_{11} = E(r_t r_{t-15})$	0.08 (0.05)	0.03 (0.04)	0.30 (0.03)	0.02 (0.01)	0.08 (0.02)	0.35 (0.00)
$m_{12} = E(r_t^2 r_{t-20}^2)$	0.15 (0.11)	0.15 (0.08)	0.52 (0.06)	0.04 (0.03)	0.18 (0.03)	0.80 (0.01)
$m_{13} = E(r_t r_{t-20})$	0.08 (0.05)	0.03 (0.04)	0.30 (0.03)	0.02 (0.01)	0.08 (0.02)	0.35 (0.00)
$m_{14} = E(r_t^2 r_{t-25}^2)$	0.14 (0.11)	0.15 (0.08)	0.52 (0.06)	0.04 (0.03)	0.17 (0.03)	0.79 (0.01)
$m_{15} = E(r_t r_{t-25})$	0.08 (0.05)	0.03 (0.03)	0.30 (0.03)	0.02 (0.01)	0.08 (0.01)	0.35 (0.00)

Values in parentheses are the standard deviations

autocovariances provide enough discriminating power for efficient estimation of the underlying parameters.²

² Following the suggestion of one of the reviewers, we have also investigated the sensitivity of the moments on the parameters over a larger range of variation of parameter values. Pertinent plots confirm that all moments show systematic variation with the three parameter values, with the only exception being m_2

Table 3 Grid points in three-dimensional contour plot

	Label	Grid points	Step size
Bimodal	σ_f	$6.00 \times 10^{-3} + i \times h$	$h = 1.50 \times 10^{-3}, i = 0, \dots, 40$
	a	$6.00 \times 10^{-5} + i \times h$	$h = 1.50 \times 10^{-5}, i = 0, \dots, 40$
	b	$2.80 \times 10^{-4} + i \times h$	$h = 7.00 \times 10^{-5}, i = 0, \dots, 40$
Unimodal	σ_f	$6.00 \times 10^{-3} + i \times h$	$h = 1.50 \times 10^{-3}, i = 0, \dots, 40$
	a	$2.80 \times 10^{-4} + i \times h$	$h = 7.00 \times 10^{-5}, i = 0, \dots, 40$
	b	$6.00 \times 10^{-5} + i \times h$	$h = 1.50 \times 10^{-5}, i = 0, \dots, 40$

Next, to reveal the surface properties of the objective function, three-dimensional contour plots of the objective value with respect to pairs of the parameters are plotted. Table 3 lists the grid points of each set of varied parameters. Parameters not varied in the plots are set equal to their default values of Table 1. In total, there are three combinations of the parameter pairs for each case.

Figure 2 plots the contour figures using the identity matrix as weighting matrix and the first seven moment conditions of Table 2. The surface of the objective function exhibits similarities for the bimodal and unimodal setting. While the surfaces appear in general relatively smooth, we sometimes see discontinuities as they would be expected under a simulation approach, especially for the plot of a versus b . In addition, there are relatively flat regions around the minimum in the plots of σ_f versus a and σ_f versus b , suggesting a potential problem of identifying the global minimum of the objective function. There are also long valleys in the plots of σ_f versus a and σ_f versus b , implying strong correlation between these parameters in certain parts of their admissible space. Note that since analytical moments have been derived in Alfaro et al. (2008) and Ghonghadze and Lux (2016), we can exclude strict collinearity. Nevertheless, the apparent proximity to collinear behavior (or weak identification) will be a major concern in our subsequent explorations. Figure 3 plots the same contours using the inverse of the Newey–West estimator of the covariance matrix of the difference between the simulated and the pseudo-empirical moments as the weighting matrix. The surfaces still are non-smooth very much like in the case of the identity weighting matrix. Some contour plots appear even somewhat more spiky than before. The surface also still exhibits flat valleys of the objective function. We also note that when increasing T_{sim} , the surface becomes increasingly smooth as demonstrated by Fig. 4 which plots the same contour plots using an identity matrix with 80,000 simulated data points. Asymptotically, we thus approach the smooth behavior of analytical moments, but should have to cope with relatively flat ridges indicating little variation of the objective function along certain dimensions. We also note that the pronounced bimodality of the surface of a versus b in Fig. 2 has vanished for $T_{sim} = 80,000$.

The irregular and non-smooth surface of the objective function creates challenges for the estimation. Standard optimization techniques utilizing derivatives are not suit-

Footnote 2 continued

under variation of a and b . Those moments for which analytical approximations exist, are also close to their analytical counterparts. Details are available upon request.

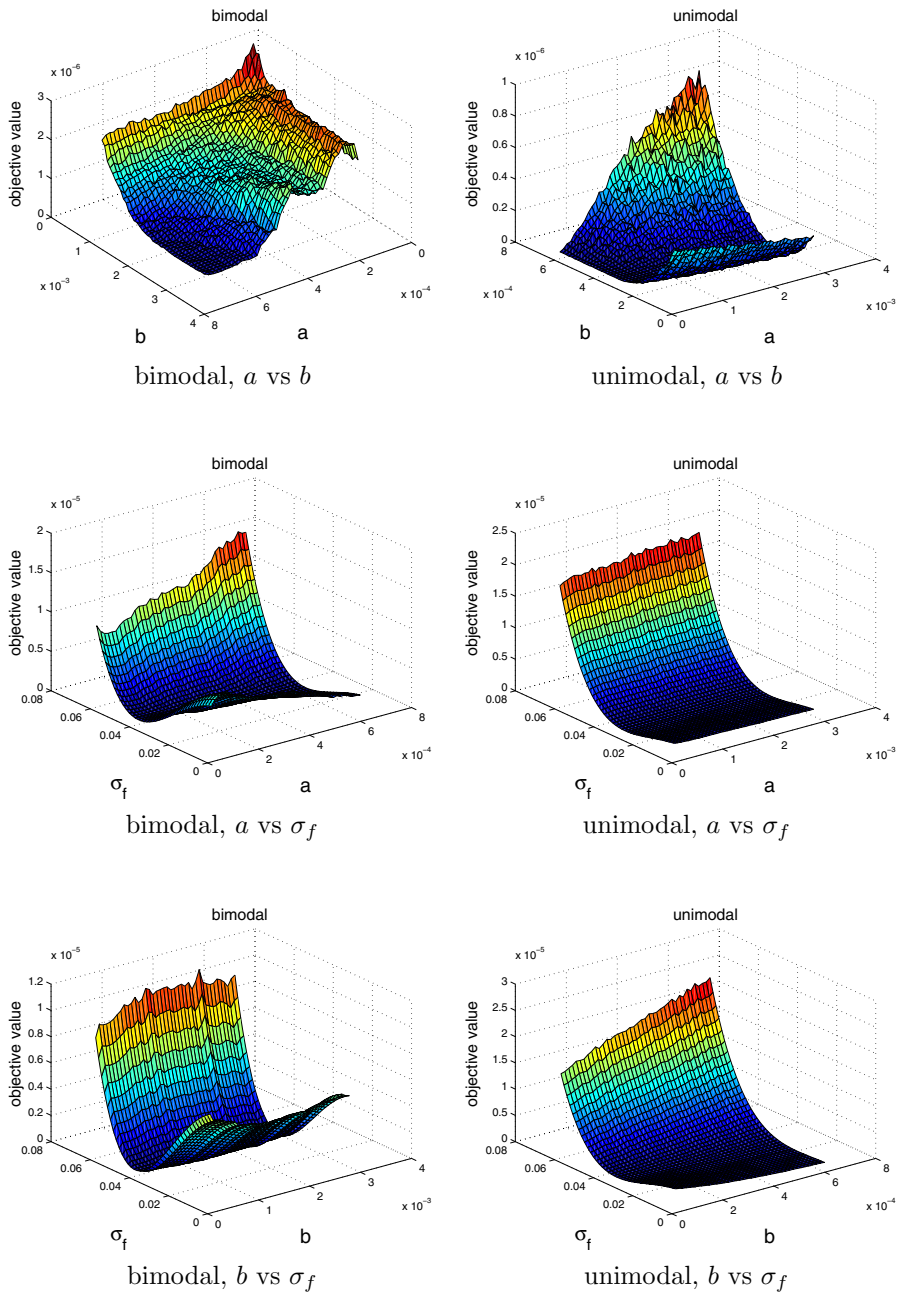


Fig. 2 3-D contour plots of the objective function for the identity matrix used as weighting matrix. Simulated data size is $T_{sim} = 20,000$

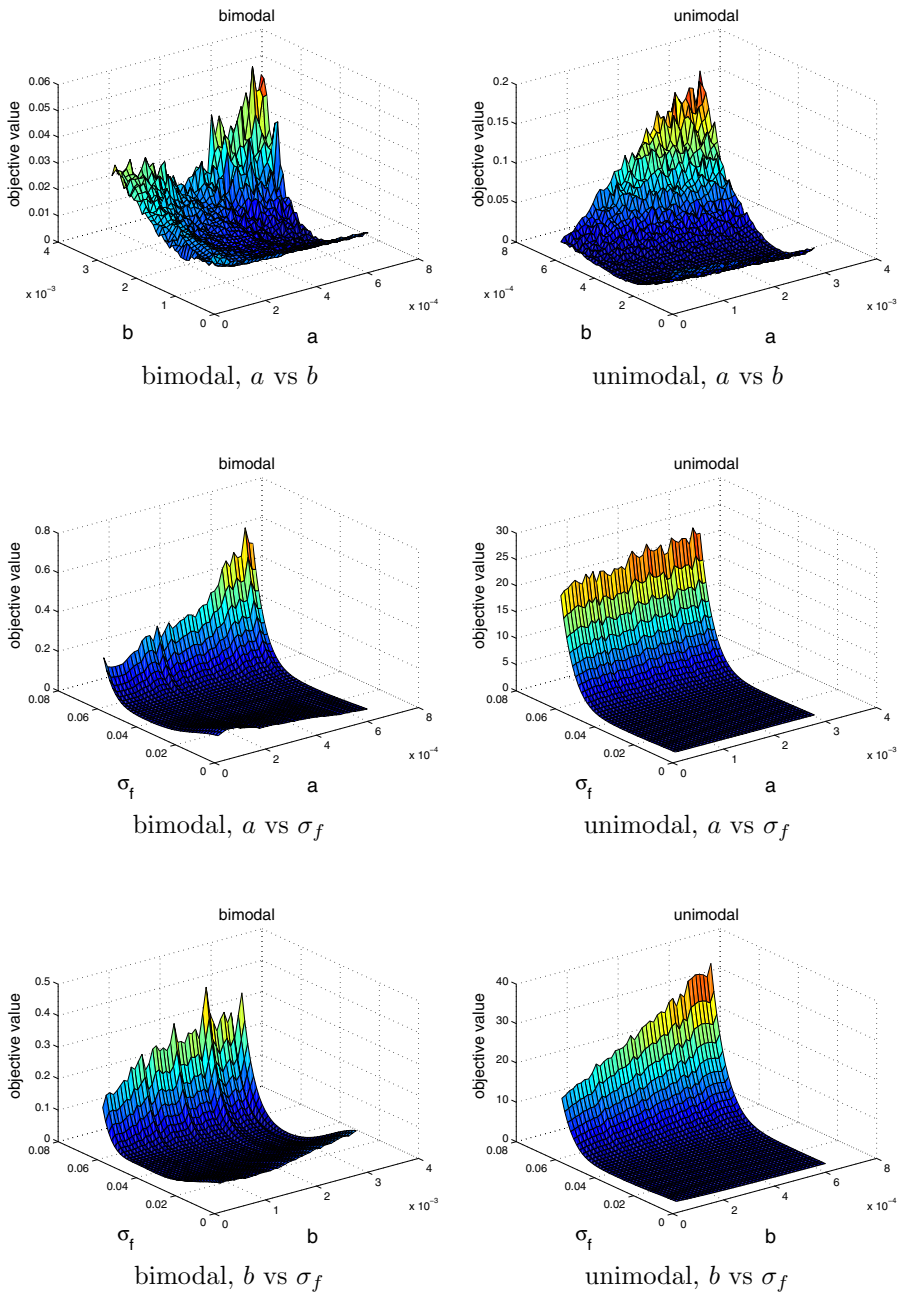


Fig. 3 3-D contour plots of the objective function for the inverse of the Newey–West estimator of the covariance of the moment conditions used as weighting matrix. Simulated data size is $T_{sim} = 20,000$

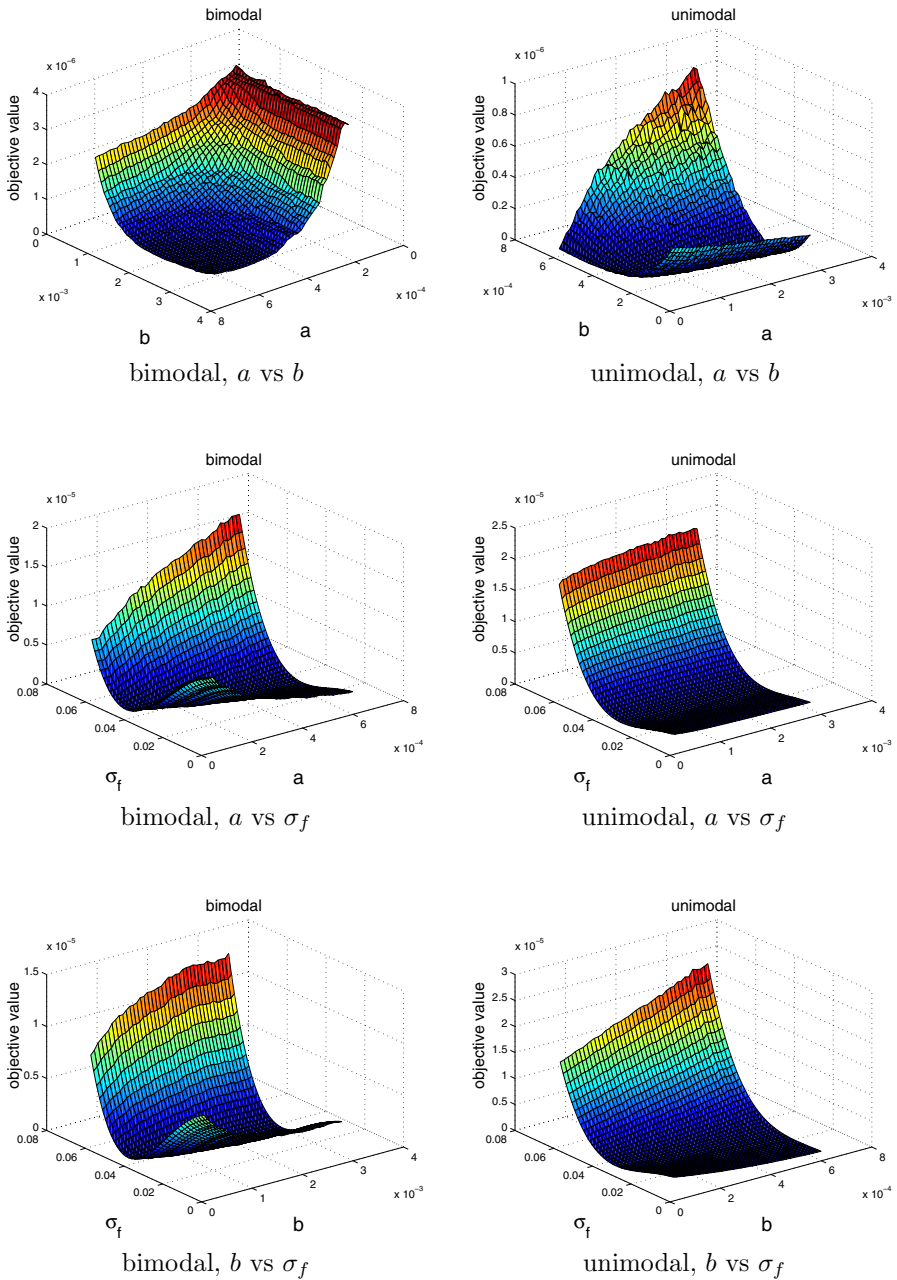


Fig. 4 3-D contour plots of the objective function for the identity matrix used as weighting matrix. Simulated data size is $T_{sim} = 80,000$

able for such problems as the derivative of the objective function is discontinuous in this case. In the following, we adopt the Nelder–Mead simplex method which is well known for being able to cope in a robust way with nonlinear optimization problems for objective functions without a smooth gradient.³

3.2 Monte Carlo Simulations

When implementing an SMM estimator for the present model, we can choose from a large range of possibilities for the moment conditions and other details of the setting. Note, that for a simulated method of moments approach, an estimator for the covariance matrix might, for instance, be based on both the simulated as well as the empirical data. Indeed, estimating the covariance matrix on the base of simulated data could be preferable since the empirical observations are limited in size whereas no such limit applies to simulated data. Hence, the covariance matrix can be estimated at a higher precision from the simulations that need to be performed anyway (cf. Carrasco and Florens 2002). To explore the performance of SMM for our simple model, we first proceeded along the classical lines of generalized moment estimators: (1) perform a first round of parameter estimation using the identity matrix as weighting matrix of the moments, (2) estimate a better weighting matrix using the inverse of the estimated covariance matrix of the moments that one obtains as a by-product of step (1), and (3) iterate the estimation process with this new weighting matrix to obtain more efficient parameter estimates.

Unfortunately, our implementation of such a relatively straightforward SMM algorithm showed very limited success initially with pertinent estimators being characterized by huge biases and standard deviations. Inspection showed that due to the lack of smoothness of the simulated objective function as shown in the previous contour plots, we have to cope with multiple local minima as well as with relatively flat surfaces in certain regions of the parameter space. Any standard optimization algorithm could, thus, not be expected to converge to a unique solution from different initial conditions. Our experiences were by and large similar to those reported by Grammig and Schaub (2014) in a similar baseline SMM approach. Different initial conditions often led to different parameter estimates that could vary quite sharply across the parameter space. The choice of suitable initial conditions prior to the optimization phase is, therefore, a critical issue. It, thus, seems indispensable to “guide” the optimization phase towards a sensible subset of the parameter space by some kind of preliminary exploration of various combinations of the parameters, and a rough mapping of the behavior of the objective function. We, therefore, modified our approach by first conducting a grid search and subsequently initiating a systematic optimization using the Nelder–Mead algorithm with the ten best grid points as initial conditions. The ‘empirical’ estimate for each such run on a test data set is, then, the parameter set with the lowest value of

³ We have also experimented with alternative, more refined optimization methods such as CMA-ES (completely derandomized self-adaptation in evolution strategies) proposed by Hansen and Ostermeier (2001), but did not find any remarkable differences in performance compared to the baseline Nelder–Mead algorithm. Many more algorithms can be tried such as, for example, the large spectrum of Bayesian optimization techniques (cf. Shahriari et al. 2016).

the objective function from the ten runs of the Nelder–Mead algorithm in phase two of the estimation. The grid points were chosen equidistantly along all three dimensions of the parameter space. We have anchored the grid around combinations of the parameters a , b and σ_f that together would yield a variance for returns equal to the one of the “pseudo-empirical” test data based on the (slightly generalized) closed-form solution derived by [Alfarano et al. \(2008\)](#):

$$\sigma_r^2 = \sigma_f^2 + \frac{4a}{2\frac{a}{b} + 1}.$$

The fundamental variation has been set equal to $\sigma_f^2 = k\sigma_r^2$ with $k = 0.1, 0.2, \dots, 0.9$ to allow for different outcomes in terms of the contribution of fundamental factors and sentiment noise to overall asset price fluctuations. In addition, a and b have been varied each over nine equidistant grid points as well, centered at the bifurcation value $\varepsilon_0 = a/b$ at which the sentiment dynamics switches from unimodal to bimodal. Setting $R = T_{sim}/T_{emp} = 4$, we run Monte Carlo simulations for $T_{emp} = 5000, 10,000, 20,000$ and $100,000$ and corresponding $T_{sim} = 20,000, 40,000, 80,000$, and $400,000$, respectively, using this design for 400 replications of any scenario. To be precise, our estimation algorithm works as follows: First, we evaluate the objective function at all 9^3 grid points using the identity matrix as the weighting matrix. We then pick the best 10 grid points, compute the weighting matrix from the variance–covariance matrix of the pertinent simulations and evoke the Nelder–Mead algorithm from those particular sets of initial values.⁴ In the Appendix 1, we provide a routine in pseudo code for our estimation approach. In Table 4, we report the results of our Monte Carlo simulations. A modified algorithm adding a second round with the new weighting matrix being determined from the parameter estimates obtained in the first round provided almost identical results and not much improvement (results are, therefore, not displayed). We report results from four different sets of moment conditions:

- SMM4 uses the following moments: unconditional second and fourth moment, first-order autocovariance of raw returns and squared returns.
- SMM7 adds three additional moments: autocovariance of absolute returns at lag 1 as well as autocovariances of squared and absolute returns at lag 5.
- SMM11 adds another four moments: the autocovariances of squared and absolute returns at lags 10 and 15.
- SMM15 adds autocovariances of squared and absolute returns at lags 20 and 25 to the previous selection of moments.

⁴ Obviously, using an extensive grid search with subsequent repeated applications of the Nelder–Mead algorithm from different starting points, we make a relatively big effort in each iteration of our Monte Carlo study to find the global optimum of the objective function. It is, however, not clear that such a computational intensive approach would be optimal for some applied purpose (e.g., using the estimated model for forecasting of volatility as in [Ghoshadze and Lux 2016](#)). A local optimum obtained with less effort might be ‘good enough’ for such a purpose, cf. [Gilli and Schumann \(2011\)](#) for a discussion of in-sample fit and out-of-sample performance in stochastic optimization problems. With respect to a portfolio choice problem, the authors demonstrate that the relationship between in-sample and out-of-sample performance is not necessarily monotonic in the computation invested to solve a numerical problem.

Table 4 Monte Carlo results for our SMM algorithms with $R = 4$ and varying T_{emp}

	SMM4			SMM7			SMM11			SMM15		
	a	b	σ_f	a	b	σ_f	a	b	σ_f	a	b	σ_f
True	0.3	1.4	30	0.3	1.4	30	0.3	1.4	30	0.3	1.4	30
$T_{emp} = 5000$												
Mean	0.57	1.45	23.03	0.48	1.47	25.72	0.47	1.41	25.85	0.48	1.33	25.59
FSSE	0.37	0.70	10.01	0.32	0.77	7.73	0.31	0.62	7.37	0.31	0.51	7.09
RMSE	0.46	0.70	12.19	0.36	0.77	8.83	0.35	0.62	8.45	0.36	0.51	8.34
$T_{emp} = 10,000$												
Mean	0.55	1.44	22.68	0.45	1.43	25.91	0.43	1.39	26.52	0.39	1.37	27.36
FSSE	0.34	0.52	9.97	0.26	0.61	6.82	0.23	0.45	5.99	0.21	0.43	5.35
RMSE	0.42	0.52	12.36	0.30	0.61	7.95	0.27	0.45	6.92	0.22	0.43	5.97
$T_{emp} = 20,000$												
Mean	0.51	1.40	23.70	0.42	1.39	26.72	0.40	1.37	27.27	0.38	1.36	27.79
FSSE	0.29	0.28	8.61	0.21	0.28	5.74	0.19	0.19	4.89	0.17	0.25	4.43
RMSE	0.36	0.28	10.66	0.24	0.28	6.60	0.21	0.19	5.59	0.18	0.25	4.95
$T_{emp} = 100,000$												
Mean	0.43	1.39	26.24	0.35	1.39	28.52	0.34	1.39	28.94	0.33	1.39	29.25
FSSE	0.20	0.09	6.14	0.11	0.09	2.96	0.09	0.08	2.52	0.08	0.09	2.30
RMSE	0.24	0.09	7.19	0.12	0.09	3.31	0.10	0.08	2.73	0.08	0.09	2.42
True	1.4	0.3	30	1.4	0.3	30	1.4	0.3	30	1.4	0.3	30
$T_{emp} = 5000$												
Mean	0.84	0.41	29.81	0.79	0.40	29.75	0.78	0.44	29.97	0.78	0.43	29.80
FSSE	0.74	0.32	4.79	0.56	0.27	4.29	0.60	0.46	4.43	0.63	0.41	4.25
RMSE	0.93	0.33	4.79	0.83	0.29	4.29	0.87	0.48	4.42	0.88	0.43	4.25
$T_{emp} = 10,000$												
Mean	0.85	0.37	30.61	0.79	0.38	30.49	0.85	0.39	30.10	0.78	0.37	30.33
FSSE	0.78	0.35	3.90	0.67	0.31	3.76	0.71	0.40	3.89	0.60	0.25	3.84
RMSE	0.96	0.35	3.94	0.90	0.31	3.78	0.90	0.41	3.89	0.86	0.26	3.85
$T_{emp} = 20,000$												
Mean	1.05	0.33	30.33	1.00	0.34	30.28	0.94	0.34	30.25	0.96	0.34	30.27
FSSE	0.86	0.11	3.25	0.88	0.10	3.23	0.80	0.11	3.23	0.84	0.11	3.30
RMSE	0.93	0.11	3.26	0.97	0.11	3.24	0.92	0.12	3.24	0.95	0.12	3.30
$T_{emp} = 100,000$												
Mean	1.32	0.30	30.55	1.47	0.30	30.35	1.51	0.30	30.26	1.45	0.30	30.37
FSSE	1.15	0.05	2.12	1.22	0.06	2.09	1.22	0.06	2.24	1.19	0.06	2.15
RMSE	1.15	0.05	2.18	1.22	0.06	2.12	1.23	0.06	2.25	1.19	0.06	2.17

Notes The table shows the means, finite sample standard errors (FSSE) and root-mean squared errors (RMSE) of 400 replications of each scenario
 Estimated parameters are multiplied by 10^3 for better readability

We might note that in all these exercises we did never apply any censoring to our estimates as it has often been done in similar Monte Carlo simulations in the literature. Hence, if the estimate of σ_f turned out to be literally 0, for instance, we did not discard it as non-sensible. The reason is that we do not have any clear prior for the parameters, and attempted to document the complete range of possibilities.

We observe the following patterns across number of moments and sample sizes: First, increasing T_{emp} , the finite sample standard deviations (FSSE) and root-mean squared errors (RMSE) mostly continue to improve for both the bimodal and unimodal settings. However, as a grain of salt, in many cases the improvement is initially slower than would be expected under \sqrt{T} consistency and only becomes pronounced at the last step from $T_{emp} = 20,000$ to 100,000. There is even one hard-nosed entry: parameter a in the unimodal scenario seems to behave in an unusual way under an increase of sample size. While its mean estimate seems to converge nicely to the ‘true’ value, its RMSE is even increasing with sample size. The reason might be that with the dominance of random idiosyncratic change of sentiment, the statistical appearance of the dynamic process is relatively insensitive to a change of this parameter within a certain bandwidth (leaving the time series behavior within the unimodal regime unchanged).

As for different moment conditions, we see different results for the two regimes: within the bimodal regime, more moments appear to enhance the precision of the estimates, with the improvement being larger when moving from four to seven than when moving on to eleven and then fifteen moment conditions. For the unimodal case we see, in fact, very little change of the results for the four different sets of moment conditions. The reason might be that with the relatively limited relevance of personal communication ($b < a$), the process also has less memory built in, and so adding more autocovariances does not help in the estimation. As has been mentioned above, adding another round of SMM based upon adopting the inverse of the covariance matrix from the parameters estimated in the first iteration as the new weighting matrix leaves results essentially unchanged and, hence, seems not worthy the computational effort.

Inspecting the details, even with such an initial grid search, we still encounter a certain number of estimates that are relatively far off the ‘true’ values in Monte Carlo runs. As we will see below, there is sizable correlation between the three parameters and far-off combinations of parameter values might generate moments that are close to the ones we obtain for a different parameter set. The adjustment of the weighting function might, therefore, not always be sufficient to leave such ‘traps’ or local valleys of the objective function. In particular, we find that there is a high negative correlation between parameters a and σ_f (i.e., sentiment and fundamental variance), and since shifting between both will lead to changes of conditional moments, (i.e., volatility persistence), additional changes in b might bring different combinations of a and σ_f in line with similar values of measures of volatility persistence. Hence, even in this very simple model, the three parameters might allow for sufficient flexibility to get close to a sample of moments with different parameter combinations.

Table 5 and Fig. 5 provide details and additional illustrations of these distortive effects present in all settings. Results here are taken from SMM7, but are pretty identical in all other variations of our SMM estimator. Table 5 shows the population

Table 5 Population correlation matrices for SMM7 with $R = 4$ and varying T_{emp}

	Bimodal			Unimodal		
	a	b	σ_f	a	b	σ_f
$T_{emp} = 5000$						
a	1	-0.27	-0.76	1	0.08	-0.71
b	-0.27	1	0.48	0.08	1	-0.32
σ_f	-0.76	0.48	1	-0.71	-0.32	1
$T_{emp} = 10,000$						
a	1	-0.22	-0.84	1	-0.01	-0.63
b	-0.22	1	0.41	-0.01	1	-0.18
σ_f	-0.84	0.41	1	-0.63	-0.18	1
$T_{emp} = 20,000$						
a	1	-0.18	-0.87	1	0.12	-0.59
b	-0.18	1	0.39	0.12	1	-0.79
σ_f	-0.87	0.39	1	-0.59	-0.79	1
$T_{emp} = 100,000$						
a	1	-0.42	-0.94	1	-0.11	-0.63
b	-0.42	1	0.58	-0.11	1	-0.65
σ_f	-0.94	0.58	1	-0.63	-0.65	1

correlation matrices for our parameter vector θ . Particularly high is the correlation between a and σ_f which we also find to increase with sample size under the bimodal setting. Similarly increasing correlation between b and σ_f is observed under the unimodal setting. Since estimates become more accurate with larger sample size, this indicates that more and more of the residual variation is due to the near-collinearity between the pertinent pairs of parameters. In contrast to the GMM implementation of [Ghonghadze and Lux \(2016\)](#), also the correlations between the second parameter of the sentiment process b and σ_f are relatively large in both scenarios. In contrast, the correlation between parameters a and b is much more moderate in both settings. Using more moments seems to help to reduce the extent of near-collinearity, but the differences between different sets of moments are relatively small. Figure 5 shows that the estimates of a suffer from a pronounced right-hand skewness (the same applies to b) while σ_f is characterized by left-hand skewness. As we can see, the range and the number of outliers decreases with sample size for both parameters a and σ_f (and also for b which is not displayed here), so that convergence to asymptotic normality seems to assert itself, albeit relatively slowly.

In Figs. 6 and 7 we exhibit the goodness-of-fit statistics obtained with the SMM parameter estimates in our Monte Carlo experiments. Namely, it is well known that the statistics $J_T = T \cdot h_T(\hat{\theta}_T)' W(\hat{\theta}_T) h_T(\hat{\theta}_T)$, i.e., T times the objective function at the estimated parameter values, $\hat{\theta}_T$, can be used to test for the validity of the hypothetical moment conditions. Under the null hypothesis that the moment conditions derived or simulated from the model are valid, the test statistics follows a χ^2 distribution with $k - l$ degrees of freedom, k being the number of moment conditions and l

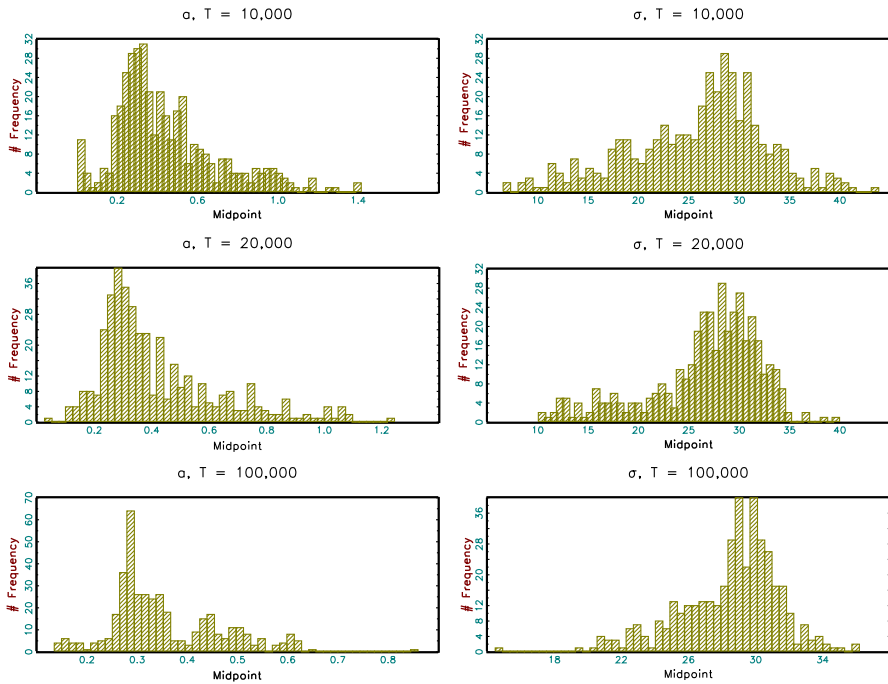


Fig. 5 SMM Monte Carlo distribution for parameter set θ of the bimodal setting, $R = 4$ and varying $Temp$ using SMM7. The *left and right panels* exhibit a and σ_f , respectively. Parameters are multiplied by 10^3 for better readability. The “true” values are $a = 0.0003$ and $\sigma_f = 0.03$

the number of estimated parameters. Figures 6 and 7 display the distribution of this statistics (known as overidentification test statistics) together with the asymptotic χ^2 distribution at all sample sizes and for all sets of moment conditions. The four moment setting ($E[r_t^2]$, $E[r_t^4]$, $E[r_t r_{t-1}]$ and $E[r_t^2 r_{t-1}^2]$) approximates the χ^2 distribution very well and the fitting of the J statistics deteriorates with the number of moments. The J-test tends to over-accept more and more with a larger number of moment conditions. The size distortion of the J test for any set of moment conditions beyond the minimal one very likely reflects the limited informational value of additional moments. The correlation of the additional moments with those already present in smaller sets, on the one hand, leads to improvements with decreasing returns, while, on the other hand, it brings in a tendency of illusory good fit.

In a number of additional simulation experiments, we tried various variations of the SMM algorithm as well as other choices of moment conditions. For instance, rather than using the identity matrix in the grid search and computing the estimate of the covariance matrix of the moment conditions based upon the best values found in the grid search, we attempted to add a data-driven initial weighting matrix in order to direct the search process toward combinations of estimates and subsequent weighting matrices that do not wander too far away from the ‘true’ values. This follows a proposal by Ghonghadze and Lux (2016) who in a companion paper on GMM estimation showed that a data-driven initial weighting matrix might reduce overall biases and variability of the estimates. However, we found little improvement within the SMM

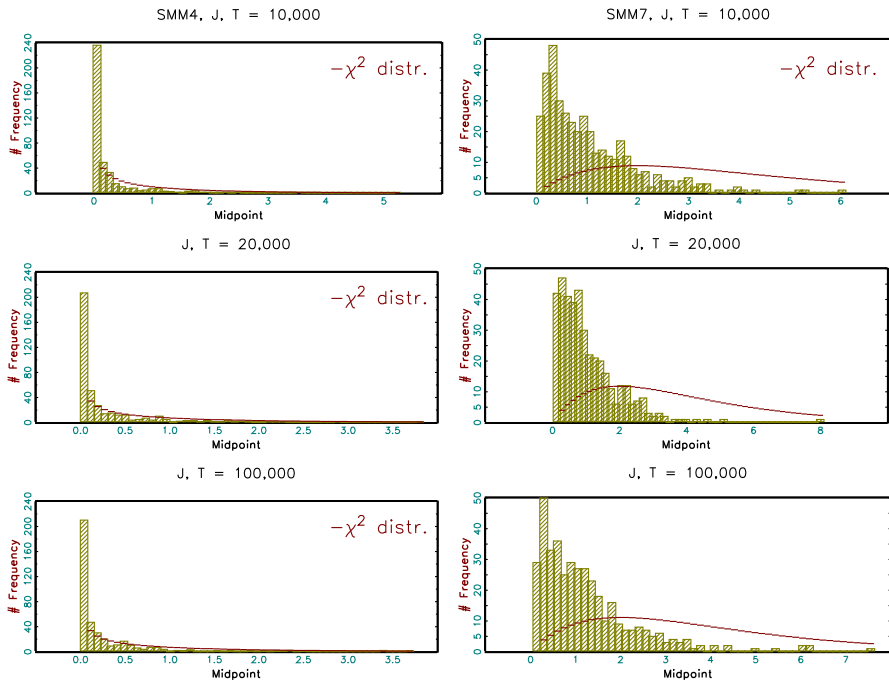


Fig. 6 Histograms of the J test statistics for validity of the underlying moment conditions together with its asymptotic χ^2 distribution under the null hypothesis for SMM4 and SMM7 for the bimodal setting, $R = 4$ and varying T_{emp}

setting. We have also tested the performance of different sets of moment conditions. For instance, we have used instead of autocovariances at single lags sums of these: $\sum_{i=1}^{50} r_t^2 r_{t-i}^2$ and $\sum_{i=51}^{100} r_t^2 r_{t-i}^2$ to hopefully better capture the decay patterns of the autocorrelation of volatility. While such moments had improved the estimations in a GMM setting (Ghonghadze and Lux 2016), here they also appear ineffective. We have also used antithetic random variables that are known to reduce the variance of simulated samples, but also this modification had no discernible effect on the quality of our estimates. Alternative estimation methods based upon evolutionary algorithms (genetic algorithms and related evolutionary approaches) did also not improve the overall outcome. As a modification to the computation of the weighting function we have computed it from the variability of the simulations alone rather than from the variability of the difference between empirical and simulated moments. All in all, however, the difference between our baseline setting and those modifications turned out to be very small and all alternative designs were inferior to the results exhibited in Table 4. It, thus, appears that the variability of moment conditions in simulations imposes certain restrictions to the quality of our estimation that cannot be overcome by any new combination of the typical information we can extract from a univariate series.

How does our SMM estimator perform vis-a-vis its Generalized Method of Moments (GMM) counterpart based on analytical moment conditions? We have attempted a comparison using the results of Ghonghadze and Lux (2016) for selected

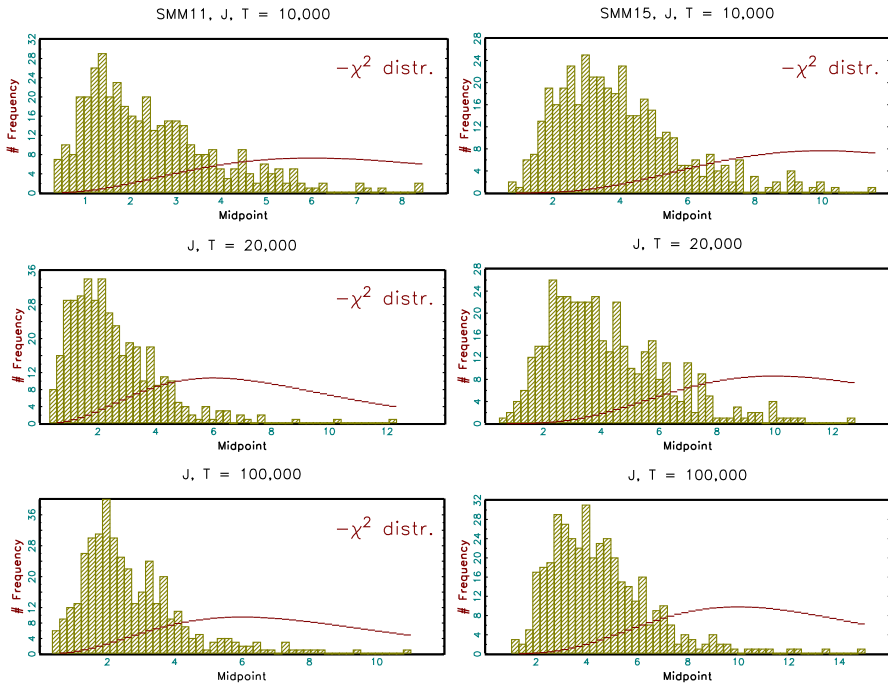


Fig. 7 Histograms of the J test statistics for validity of the underlying moment conditions together with its asymptotic χ^2 distribution under the null hypothesis for SMM11 and SMM15 for the bimodal setting, $R = 4$ and varying T_{emp}

moments. Asymptotically (in the limit of the sample size tending to infinity), the differences between both estimators are known (cf. [Duffie and Singleton 1993](#); [Carrasco and Florens 2002](#)) and they should, of course, vanish for simulated sample sizes going to infinity. If $R \rightarrow \infty$, the SMM estimator should, thus, converge to the GMM estimator in terms of the distribution of the estimates and the value of the objective function. By fixing $T_{emp} = 100,000$ and varying $R = 4, 8$ and 16 , we evaluate the effect of R on the performance of the estimation of our model for a particular set of moments. Unfortunately, [Ghoshadze and Lux \(2016\)](#) only provide results for unconditional moments as well as for autocovariances of squared returns, but not for autocovariances of absolute returns. We, thus, resort to a somewhat different set of moment conditions for the comparison using the six moments $E[r_t^2]$, $E[r_t^4]$, and $E[r_t^2 r_{t-i}^2]$ for $i = 1, 5, 10$ and 20 . The results are shown in Table 6.

For the covariance estimator, the simulation noise accounts for a factor $1/R$ “more” of variation compared to the GMM covariance of moment conditions due to the additional sampling variability brought in by the use of simulated rather than analytical moments (cf. [Duffie and Singleton 1993](#)). Choosing factors $R = 4, 8$, and 16 , our results should not be too far from those reported in [Ghoshadze and Lux \(2016\)](#). Hence, we would expect a relative efficiency of our SMM compared to a GMM estimator with the same moments of $R/(1 + R) = 0.8, 0.89$, and 0.94 for $R = 4, 8$, and 16 . The comparison between SMM and GMM estimates provides mixed results. First, when only inspecting the sequence of SMM experiments, we see slight overall

Table 6 Monte Carlo result for fixed $T_{emp} = 100,000$ and varying R

	SMM6			SMM7		
	a	b	σ_f	a	b	σ_f
True	0.3	1.4	30	0.3	1.4	30
$R = 4$						
Mean	0.38	1.39	27.75	0.35	1.39	28.52
FSSE	0.13	0.09	3.83	0.11	0.09	2.96
RMSE	0.15	0.09	4.44	0.12	0.09	3.31
$R = 8$						
Mean	0.36	1.40	28.31	0.35	1.39	28.70
FSSE	0.13	0.08	3.77	0.10	0.09	2.82
RMSE	0.14	0.08	4.13	0.11	0.09	3.10
$R = 16$						
Mean	0.36	1.39	28.32	0.34	1.39	28.84
FSSE	0.12	0.08	3.64	0.10	0.08	2.77
RMSE	0.14	0.09	4.01	0.10	0.08	3.00
GMM						
Mean	0.45	1.17	27.18			
FSSE	0.22	0.50	5.76			
RMSE	0.26	0.55	6.41			
True	1.4	0.3	30	1.4	0.3	30
$R = 4$						
Mean	1.27	0.30	30.39	1.47	0.30	30.35
FSSE	1.08	0.06	2.04	1.22	0.06	2.09
RMSE	1.08	0.06	2.08	1.22	0.06	2.12
$R = 8$						
Mean	1.29	0.31	30.34	1.55	0.30	30.20
FSSE	1.11	0.06	1.97	1.24	0.06	2.01
RMSE	1.12	0.06	2.00	1.25	0.06	2.02
$R = 16$						
Mean	1.39	0.31	30.16	1.67	0.30	30.16
FSSE	1.09	0.06	2.03	1.33	0.05	2.15
RMSE	1.08	0.06	2.03	1.35	0.05	2.15
GMM						
Mean	1.03	0.62	27.10			
FSSE	0.31	0.52	2.09			
RMSE	0.49	0.61	3.57			

Notes The table shows the means, finite sample standard errors (FSSE) and root-mean squared errors (RMSE) of 400 replications of each scenario. Estimated parameters are multiplied by 10^3 for better readability

improvements from $R = 4$ through $R = 8$ and $R = 16$ for the bimodal setting, but no clear tendency for the unimodal case. The same applies to our estimates based upon SMM7 which are shown in the right-hand part of Table 6 without GMM counterparts. Further, in comparison with the GMM estimates in the case of six moments, we

find that SMM provides uniformly better results in the bimodal case. In the unimodal setting, SMM and GMM results are hard to compare as SMM provides for a better quality on average of the fit of parameters b and σ_f , but performs worse for parameter a . It seems that there might be different factors at work that lead to different types of distortions under SMM and GMM, respectively. The better performance of SMM in at least the bimodal setting might indicate that with an immense effort in terms of simulation time and a large enough empirical sample, simulated moments could become so precise that they could improve upon the approximations employed in the GMM approach of [Ghoshadze and Lux \(2016\)](#). Note, however, that we observed such a convenient performance of SMM vis-à-vis GMM only for the large sample size of $T_{emp} = 100,000$. With smaller pseudo-empirical samples (reported in the working paper version) SMM did not recognizably converge to the precision of SMM.

4 Empirical Application

In this section, we apply the approach developed in the previous parts of this paper to estimate our model for a number of financial asset indices and prices. The selected empirical datasets include three stock market indices, three foreign exchange rates and the price of gold, all extracted from Datastream. The stock market indices are: the German DAX, the S&P 500, and the Japanese Nikkei. The foreign exchange rates are: U.S. dollar to euro (USD/EUR), Japanese yen to U.S. dollar (YEN/USD) and Swiss franc to euro (CHF/EUR). The three stock indices and the gold price use daily data with sample period from 01/01/1980 to 12/31/2005. Data for the foreign exchange rates include periods 01/01/1999 to 12/31/2010 (USD/EUR), 01/02/1986 to 12/31/2005 (YEN/USD) and 07/15/2003 to 12/31/2010 (CHF/EUR). We use the above sets of 4, 7, 11 and 15 moments in the estimation with one round of optimization. For the simulations, we set $R = 4$, i.e., $T_{sim} = 4 \cdot T_{emp}$. Table 7 shows the estimated results.

Overall, the four algorithms lead to mostly comparable results for each time series, and also the orders of magnitude of the three parameters are often within the same range across the different assets. Except for the interaction parameter b in the case of the CHF/EUR exchange rate and σ_f under the setting of SMM4 for S&P 500, all parameters are highly significant under all algorithms and for all time series. Furthermore, in all cases except for the CHF/EUR, it holds that $a < b$, i.e. in the light of our model returns appear to be driven by a mixture of fundamentals and sentiment with the later entailing a strong contagion component. The contribution of sentiment to overall volatility implied by the pertinent parameter estimates is shown in the last column. Its range is from 27 to 91% with foreign exchange markets showing typically the lowest values followed by the stock markets and finally by gold with a maximum ratio of non-fundamental influences. This ranking agrees nicely with received wisdom on which types of markets are prone more or less to speculative factors and fluctuations of sentiment. Save for three out of twenty-eight cases the J test does not reject the null hypothesis that the empirical moments all have been generated by our model. This statement has, of course, to be seen in the light of the size distortion of the J test for the settings with 7, 11 and 15 moments.

Table 7 J-test and estimated parameters

	J	$a \times 10^3$	$b \times 10^3$	$\sigma_f \times 10^3$	Rel. Var
DAX					
SMM4	0.01 (0.92)	0.07*** (0.00)	0.58*** (0.02)	9.12*** (0.83)	0.53
SMM7	1.92 (0.75)	0.04*** (0.00)	0.61*** (0.01)	10.41*** (0.55)	0.38
SMM11	3.97 (0.86)	0.05*** (0.00)	0.37*** (0.01)	9.63*** (0.42)	0.47
SMM15	3.76 (0.99)	0.05*** (0.00)	0.44*** (0.01)	9.77*** (0.40)	0.46
S&P 500					
SMM4	0.63 (0.43)	0.07** (0.04)	0.24*** (0.09)	3.11 (2.34)	0.91
SMM7	2.17 (0.70)	0.06*** (0.00)	0.33*** (0.01)	5.80*** (0.43)	0.69
SMM11	11.39 (0.18)	0.04*** (0.00)	0.21*** (0.00)	6.66*** (0.33)	0.59
SMM15	8.36 (0.76)	0.04*** (0.00)	0.14*** (0.00)	7.04*** (0.24)	0.55
Nikkei					
SMM4	1.09 (0.30)	0.10*** (0.01)	0.17*** (0.02)	6.73*** (0.86)	0.72
SMM7	0.71 (0.95)	0.08*** (0.00)	0.26*** (0.02)	7.20*** (0.49)	0.67
SMM11	1.58 (0.99)	0.08*** (0.00)	0.25*** (0.01)	7.36*** (0.35)	0.66
SMM15	1.89 (1.00)	0.08*** (0.00)	0.24*** (0.01)	7.09*** (0.34)	0.68
USD/EUR					
SMM4	0.46 (0.50)	0.05*** (0.01)	0.00*** (0.00)	5.40*** (0.22)	0.28
SMM7	7.98* (0.09)	0.01*** (0.00)	0.01*** (0.00)	5.25*** (0.16)	0.32
SMM11	8.70 (0.37)	0.01*** (0.00)	0.09*** (0.00)	5.25*** (0.15)	0.32
SMM15	13.56 (0.33)	0.01*** (0.00)	0.13*** (0.00)	5.54*** (0.13)	0.24

Table 7 continued

	J	$a \times 10^3$	$b \times 10^3$	$\sigma_f \times 10^3$	Rel. Var
YEN/USD					
SMM4	0.13 (0.72)	0.04*** (0.00)	0.15*** (0.00)	4.46*** (0.58)	0.62
SMM7	1.90 (0.76)	0.02*** (0.00)	0.08*** (0.00)	5.38*** (0.34)	0.44
SMM11	4.99 (0.76)	0.01*** (0.00)	0.08*** (0.00)	5.34*** (0.13)	0.45
SMM15	6.72 (0.88)	0.03*** (0.00)	0.12*** (0.00)	5.40*** (0.13)	0.44
CHF/EUR					
SMM4	2.10 (0.15)	0.01*** (0.00)	0 (0.00)	2.40*** (0.20)	0.41
SMM7	3.24 (0.52)	0.00*** (0.00)	0 (0.00)	2.37*** (0.19)	0.42
SMM11	3.62 (0.89)	0.00*** (0.00)	0 (0.00)	2.42*** (0.16)	0.40
SMM15	5.61 (0.93)	0.00*** (0.00)	0 (0.00)	2.40*** (0.14)	0.40
Gold					
SMM4	2.07 (0.15)	0.08*** (0.01)	0.57*** (0.17)	3.91 (3.72)	0.89
SMM7	3.25 (0.52)	0.07*** (0.00)	0.47*** (0.01)	4.92*** (1.65)	0.83
SMM11	22.11*** (0.01)	0.05*** (0.00)	0.24*** (0.01)	5.89*** (0.41)	0.75
SMM15	25.83** (0.01)	0.07*** (0.00)	0.01*** (0.00)	6.92*** (0.35)	0.65

Values in parentheses are the asymptotic p-value for the J-test and standard errors for the three parameters. The last column measures the fraction of the variance of returns attributed to the sentiment changes as implied by the pertinent parameter estimates

*, **, and *** Stand for 10, 5 and 1% significance level

5 Conclusion

We have investigated simulated method of moment estimation of the model of [Alfarano et al. \(2008\)](#), a simple equilibrium asset pricing model based on the interplay of fundamental factors and a nonlinear sentiment process among the noise traders.

Due to the stochastic nature of simulated moments, the objective function has discontinuous derivatives and a partially very flat surface, implying multiple local minima of the objective function and identification problems. These challenges render the classical simulated moment estimator unsatisfactory as even with long data sets we observe strong sensitivity of estimation results on the starting values for the optimization. To

tackle these challenges, we develop a systematic approach embedding a grid search phase for initialization followed by systematic SMM estimation. In our SMM estimation, we compared a variety of settings. As it turned out a standard SMM setting with Newey–West weight matrix performs best when initiated with a systematic grid search. Without such a grid search, the outcome of estimation based on any arbitrary set of initial conditions might just be any of a large set of local minima (very much as in the experiments by [Grammig and Schaub 2014](#)). As a consequence, any single estimation results reported in the literature for the present or related agent-based models would have to be interpreted with caution. Various more “exotic” choices of weighting matrix and optimization scheme did not improve our estimates. Using more elementary moments did enhance precision, but with decreasing marginal returns. Additionally, the somewhat better estimates come at the cost of size distortions of the J test. Using more elaborate moment conditions did not improve results, and the same applies for a second iteration of the SMM algorithm with a new weighting matrix based on the first-round estimates.

We also find that the inherent simulation noise provides some principal limitations to the precision of parameter estimates even of a simple model like the present one. Since applicability of asymptotic theory is guaranteed in the present setting, we conclude that much more data is required than typically available for financial markets to reach the realm of, for instance, \sqrt{T} scaling of errors or relative efficiency of SMM against GMM as predicted by theory. This is also in line with recent findings by [Grammig and Schaub \(2014\)](#) for a different type of asset-pricing model. The reason for this slow improvement of the quality of an estimator with both increasing sample size and increasing size of simulations might be the very nature of the time series and their stylized facts. It is well-known, for example, that also the confidence intervals of tail index estimates are much wider in the presence of heteroskedasticity than predicted by asymptotic theory ([Kearns and Pagan 1997](#)). Since the tail index averages over the extremal part of a density (e.g., the highest 10% of observations), it might already be expected to have smaller errors than the single moments used in our setting. Hence, the slowing convergence rates that we observed for our various SMM estimators might have their source in the very nature of the stylized facts that the present model and similar ones attempt to capture. Precision of univariate asset pricing models via (simulated) moment matching might, thus, face some principal limitations.

Acknowledgements We gratefully acknowledge funding from the European Union’s Seventh Framework Programme under Grant Agreement No. 612955. Helpful comments by Reiner Franke, Simone Alfarano, two anonymous reviewers and participants at various seminars and conference presentations are thankfully acknowledged as well.

Appendix 1: Pseudo Code

Below is the pseudo code for the SMM Monte Carlo simulations.

Algorithm: SMM Monte Carlo simulations

```

1: for i = 1 to 400, do
2:   Set random seed 1: seed1(i).
3:   Generate pseudo-empirical time series with sample size  $T_{emp}$ .
4:   Set random seed 2: seed2(i).
5:   Set weighting matrix  $W1$  equal to identity matrix.
6:   Grid search to find 10 best parameter sets  $\theta_k, k = 1, \dots, 10$ .
7:   for  $k = 1$  to 10, do
8:     Based on  $\theta_k$ , simulate time series with sample size  $T_{sim}$  and calculate weighting matrix  $W2$ 
       using Newey West estimator.
9:     Minimize the objective function to obtain the optimized parameter  $\hat{\theta}_k$ .
10:   end for
11:   Output the best optimized parameter set among the 10 optimized  $\hat{\theta}_k$ .
12: end for

```

Appendix 2: Tests for Stationarity and Ergodicity

We follow the runs test procedure of [Grazzini \(2012\)](#) to test the stationarity and ergodicity of the sentiment dynamics and raw returns from the agent based model as well as the generated moments. For the stationarity test, we generate a time series with sample size 2,000,000 and adopt the runs test procedures with different test window lengths 1, 10, 50, 100, 500, 1000, 5000 and 10,000. We repeat the test for 100 runs. As reported in Table 8, under the bimodal setting, the probabilities of rejecting stationarity at the level of 5% are much higher than 0.05 for the second and fourth moment and the autocovariances of squared returns for small test windows. Increasing the test window, probabilities of rejection of stationarity decrease towards their nominal size. It can be concluded that sentiment, raw returns as well as all the moment conditions are stationary but for the second and fourth moment and autocovariances of squared returns, the long-range dependence of volatility makes smaller samples appear non-stationary. Similar results can be found under the unimodal setting.

For the ergodicity test, we generate time series with different sample sizes 5000, 10,000, 20,000, 100,000 and 200,000. We divide these time series into 100 sub-samples to create the first test sample. Matching the sample size of these sub-samples, we also generate 100 time series (with different random seeds) to create the second test sample. The two test samples are used to test the ergodicity property of the sentiment index x_t , raw returns and the 15 moment conditions. We again repeat the test 100 times. Table 9 reports the result of the ergodicity tests. Regardless of the parameter values, the number of rejections is smaller than the nominal size of the test for raw returns and all the moment conditions. For sentiment, we find sizable numbers of rejections for smaller sample size reflecting the strong autocorrelation of this variable.

Table 8 Stationarity tests with sample size of 2 million for different sizes of test windows

Test window	Bimodal						Unimodal									
	1	10	50	100	500	1000	5000	10,000	1	10	50	100	500	1000	5000	10,000
x_t	1.00	1.00	1.00	1.00	1.00	1.00	0.79	0.16	1.00	1.00	1.00	1.00	1.00	1.00	0.11	0.08
r_t	0.24	0.25	0.08	0.18	0.37	0.63	0.28	0.10	0.08	0.32	0.86	0.99	0.96	0.68	0.05	0.13
$m_1 = E(r_t^2)$	1.00	1.00	1.00	1.00	1.00	0.99	0.06	0.02	0.12	0.96	1.00	1.00	0.38	0.11	0.03	0.05
$m_2 = E(r_t r_{t-1})$	0.32	0.06	0.05	0.06	0.02	0.10	0.07	0.06	0.16	0.07	0.06	0.06	0.05	0.04	0.05	0.08
$m_3 = E(r_t^2 r_{t-1}^2)$	1.00	1.00	1.00	1.00	1.00	1.00	0.10	0.03	1.00	1.00	1.00	0.96	0.21	0.07	0.09	0.02
$m_4 = E\left(r_t^4\right)$	1.00	1.00	1.00	1.00	1.00	1.00	0.06	0.03	0.21	0.92	1.00	0.98	0.24	0.05	0.05	0.03
$m_5 = E(r_t r_{t-1})$	1.00	1.00	1.00	1.00	1.00	0.99	0.03	0.07	1.00	1.00	1.00	0.99	0.28	0.09	0.04	0.05
$m_6 = E(r_t^2 r_{t-5}^2)$	1.00	1.00	1.00	1.00	1.00	0.99	0.05	0.05	0.32	1.00	1.00	1.00	0.20	0.07	0.06	0.07
$m_7 = E(r_t r_{t-5})$	1.00	1.00	1.00	1.00	1.00	1.00	0.04	0.09	0.32	1.00	1.00	1.00	0.33	0.13	0.04	0.05
$m_8 = E(r_t^2 r_{t-10}^2)$	1.00	1.00	1.00	1.00	1.00	0.99	0.05	0.04	0.40	1.00	1.00	1.00	0.20	0.06	0.08	0.02
$m_9 = E(r_t r_{t-10})$	1.00	1.00	1.00	1.00	1.00	0.98	0.06	0.03	0.34	1.00	1.00	1.00	0.37	0.08	0.07	0.04
$m_{10} = E(r_t^2 r_{t-15}^2)$	1.00	1.00	1.00	1.00	1.00	0.99	0.06	0.04	0.40	1.00	1.00	1.00	0.26	0.07	0.03	0.05
$m_{11} = E(r_t r_{t-15})$	1.00	1.00	1.00	1.00	1.00	0.99	0.03	0.07	0.31	1.00	1.00	1.00	0.38	0.17	0.06	0.04
$m_{12} = E(r_t^2 r_{t-20}^2)$	1.00	1.00	1.00	1.00	1.00	0.99	0.05	0.03	0.35	0.95	1.00	1.00	0.33	0.05	0.05	0.05
$m_{13} = E(r_t r_{t-20})$	1.00	1.00	1.00	1.00	1.00	1.00	0.07	0.07	0.33	0.96	1.00	1.00	0.37	0.10	0.05	0.02
$m_{14} = E(r_t^2 r_{t-25}^2)$	1.00	1.00	1.00	1.00	1.00	0.99	0.07	0.05	0.37	0.95	1.00	1.00	0.34	0.10	0.08	0.05
$m_{15} = E(r_t r_{t-25})$	1.00	1.00	1.00	1.00	1.00	1.00	0.07	0.06	0.34	1.00	1.00	1.00	0.48	0.10	0.01	0.04

The reported values are the fractions of rejections of stationarity for 100 runs

Table 9 Ergodicity tests for different sample sizes

Sample size	Bimodal					Unimodal				
	5000	10,000	20,000	100,000	200,000	5000	10,000	20,000	100,000	200,000
x_t	0.75	0.44	0.16	0.06	0.03	0.19	0.17	0.06	0.11	0.07
r_t	0.00	0.01	0.01	0.00	0.00	0.01	0.01	0.01	0.00	0.04
$m_1 = E(r_t^2)$	0.03	0.00	0.00	0.01	0.00	0.01	0.00	0.01	0.01	0.00
$m_2 = E(r_t r_{t-1})$	0.02	0.00	0.00	0.00	0.00	0.00	0.00	0.00	0.02	0.02
$m_3 = E(r_t^2 r_{t-1}^2)$	0.02	0.02	0.00	0.00	0.01	0.00	0.02	0.00	0.00	0.00
$m_4 = E\left(r_t^4\right)$	0.02	0.01	0.02	0.01	0.00	0.00	0.01	0.00	0.01	0.00
$m_5 = E(r_t r_{t-1})$	0.01	0.00	0.00	0.00	0.00	0.00	0.00	0.00	0.00	0.04
$m_6 = E(r_t^2 r_{t-5}^2)$	0.03	0.00	0.00	0.00	0.00	0.00	0.00	0.00	0.00	0.01
$m_7 = E(r_t r_{t-5})$	0.02	0.01	0.01	0.03	0.01	0.00	0.00	0.01	0.00	0.00
$m_8 = E(r_t^2 r_{t-10}^2)$	0.04	0.02	0.01	0.00	0.00	0.02	0.00	0.02	0.00	0.00
$m_9 = E(r_t r_{t-10})$	0.01	0.04	0.00	0.00	0.00	0.00	0.00	0.00	0.01	0.00
$m_{10} = E(r_t^2 r_{t-15}^2)$	0.00	0.00	0.00	0.01	0.03	0.00	0.00	0.03	0.00	0.01
$m_{11} = E(r_t r_{t-15})$	0.04	0.01	0.01	0.01	0.01	0.00	0.01	0.00	0.01	0.00
$m_{12} = E(r_t^2 r_{t-20}^2)$	0.02	0.00	0.02	0.00	0.02	0.01	0.00	0.01	0.00	0.00
$m_{13} = E(r_t r_{t-20})$	0.02	0.00	0.01	0.01	0.00	0.02	0.00	0.00	0.00	0.00
$m_{14} = E(r_t^2 r_{t-25}^2)$	0.04	0.01	0.00	0.03	0.01	0.00	0.01	0.02	0.00	0.00
$m_{15} = E(r_t r_{t-25})$	0.02	0.02	0.00	0.00	0.00	0.00	0.00	0.00	0.00	0.01

The reported values are the fractions of rejections of ergodicity for 100 runs

References

- Alfarano, S., & Lux, T. (2007). A noise trader model as a generator of apparent financial power laws and long memory. *Macroeconomic Dynamics*, 11(S1), 80–101.
- Alfarano, S., Lux, T., & Wagner, F. (2005). Estimation of agent-based models: The case of an asymmetric herding model. *Computational Economics*, 26(1), 19–49.
- Alfarano, S., Lux, T., & Wagner, F. (2008). Time variation of higher moments in a financial market with heterogeneous agents: An analytical approach. *Journal of Economic Dynamics and Control*, 32(1), 101–136.
- Barde, S. (2016). Direct calibration and comparison of agent-based herding models of financial markets. *Journal of Economic Dynamics and Control*, 73, 329–353.
- Brock, W. A., & Hommes, C. H. (1998). Heterogeneous beliefs and routes to chaos in a simple asset pricing model. *Journal of Economic Dynamics and Control*, 22(8–9), 1235–1274.
- Brown, G. W., & Cliff, M. T. (2004). Investor sentiment and the near-term stock market. *Journal of Empirical Finance*, 11(1), 1–27.
- Carrasco, M., & Florens, J.-P. (2002). Simulation-based method of moments and efficiency. *Journal of Business and Economic Statistics*, 20(4), 482–492.
- Chiarella, C., & He, X.-Z. (2002). Heterogeneous beliefs, risk and learning in a simple asset pricing model. *Computational Economics*, 19(1), 95–132.
- Day, R. H., & Huang, W. (1990). Bulls, bears and market sheep. *Journal of Economic Behavior and Organization*, 14(3), 299–329.
- De Grauwe, P., Dewachter, H., & Embrechts, M. (1995). *Exchange rate theory: Chaotic models of foreign exchange markets*. Oxford: Blackwell.
- Duffie, D., & Singleton, K. J. (1993). Simulated moments estimation of Markov models of asset prices. *Econometrica*, 61(4), 929–952.
- Ethier, S., & Kurtz, T. (1986). *Markov processes: Characterization and convergence*. New York: Wiley.
- Franke, R. (2009). Applying the method of simulated moments to estimate a small agent-based asset pricing model. *Journal of Empirical Finance*, 16(5), 804–815.
- Franke, R., & Westerhoff, F. (2011). Estimation of a structural stochastic volatility model of asset pricing. *Computational Economics*, 38(1), 53–83.
- Franke, R., & Westerhoff, F. (2012). Structural stochastic volatility in asset pricing dynamics: Estimation and model contest. *Journal of Economic Dynamics and Control*, 36(8), 1193–1211.
- Franke, R., & Westerhoff, F. (2016). Why a simple herding model may generate the stylized facts of daily returns: Explanation and estimation. *Journal of Economic Interaction and Coordination*, 11(1), 1–34.
- Ghoshghadze, J., & Lux, T. (2016). Bringing an elementary agent-based model to the data: Estimation via GMM and an application to forecasting of asset price volatility. *Journal of Empirical Finance*, 37, 1–19.
- Gilli, M., & Schumann, E. (2011). Optimal enough? *Journal of Heuristics*, 17(4), 373–387.
- Gilli, M., & Winker, P. (2003). A global optimization heuristic for estimating agent based models. *Computational Statistics & Data Analysis*, 42(3), 299–312.
- Grammig, J., & Schaub, E.-M. (2014). Give me strong moments and time: Combining GMM and SMM to estimate long-run risk asset pricing models (July 22, 2014). CFS Working Paper No. 479. Available at SSRN: <http://ssrn.com/abstract=2508125> or <http://dx.doi.org/10.2139/ssrn.2508125>.
- Grazzini, J. (2012). Analysis of the emergent properties: Stationarity and ergodicity. *Journal of Artificial Societies and Social Simulation*, 15(2), 7.
- Grazzini, J., & Richiardi, M. (2015). Estimation of ergodic agent-based models by simulated minimum distance. *Journal of Economic Dynamics and Control*, 51, 148–165.
- Hansen, N., & Ostermeier, A. (2001). Completely derandomized self-adaptation in evolution strategies. *Evolutionary Computation*, 9(2), 159–195.
- Hommes, C. H. (2006). Heterogeneous agent models in economics and finance. In L. Tesfatsion & K. Judd (Eds.), *Handbook of computational economics* (Vol. 2, pp. 1109–1186). Amsterdam: Elsevier.
- Jang, T.-S. (2015). Identification of social interaction effects in financial data. *Computational Economics*, 45(2), 207–238.
- Kearns, P., & Pagan, A. (1997). Estimating the density tail index for financial time series. *Review of Economics and Statistics*, 79(2), 171–175.
- Kirman, A. (1993). Ants, rationality, and recruitment. *Quarterly Journal of Economics*, 108(1), 137–156.

- Lamperti, F. (2015). An information theoretic criterion for empirical validation of time series models. LEM Working Papers Series 2015/02, Sant'Anna School of Advanced Studies, Pisa, Italy.
- Larsen, K. S., & Sørensen, M. (2007). Diffusion models for exchange rates in a target zone. *Mathematical Finance*, 17(2), 285–306.
- LeBaron, B. (2006). Agent-based computational finance. In L. Tesfatsion & K. Judd (Eds.), *Handbook of computational economics* (Vol. 2, pp. 1187–1233). Amsterdam: Elsevier.
- Lee, B.-S., & Ingram, B. F. (1991). Simulation estimation of time-series models. *Journal of Econometrics*, 47(2–3), 197–205.
- Lux, T. (1995). Herd behaviour, bubbles and crashes. *Economic Journal*, 105(431), 881–896.
- Lux, T. (2009a). Rational forecasts or social opinion dynamics? Identification of interaction effects in a business climate survey. *Journal of Economic Behavior & Organization*, 72(2), 638–655.
- Lux, T. (2009b). Stochastic behavioral asset-pricing models and the stylized facts. In T. Hens & K. R. Schenk-Hoppé (Eds.), *Handbook of financial markets: Dynamics and evolution* (pp. 161–215). San Diego: North-Holland.
- Manzan, S., & Westerhoff, F. (2005). Representativeness of news and exchange rate dynamics. *Journal of Economic Dynamics and Control*, 29(4), 677–689.
- McFadden, D. (1989). A method of simulated moments for estimation of discrete response models without numerical integration. *Econometrica*, 57(5), 995–1026.
- Molina, G., Bayarri, M. J., & Berger, J. O. (2005). Statistical inverse analysis for a network microsimulator. *Technometrics*, 47(4), 388–398.
- Pakes, A., & Pollard, D. (1989). Simulation and the asymptotics of optimization estimators. *Econometrica*, 57(5), 1027–1057.
- Rahmandad, H., & Sabounchi, N. (2012). Modeling and estimating individual and population obesity dynamics. In S. Yang, A. Greenberg, & M. Endsley (Eds.), *Social Computing, Behavioral—Cultural Modeling and Prediction, Volume 7227 of Lecture Notes in Computer Science* (pp. 306–313). Berlin: Springer.
- Ruge-Murcia, F. J. (2007). Methods to estimate dynamic stochastic general equilibrium models. *Journal of Economic Dynamics and Control*, 31(8), 2599–2636.
- Shahriari, B., Swersky, K., Wang, Z., Adams, R. P., & de Freitas, N. (2016). Taking the human out of the loop: A review of Bayesian optimization. *Proceedings of the IEEE*, 104(1), 148–175.
- Winker, P., Gilli, M., & Jeleskovic, V. (2007). An objective function for simulation based inference on exchange rate data. *Journal of Economic Interaction and Coordination*, 2(2), 125–145.